$(Fe, Co)_{16}N_2$ films with high saturation magnetization prepared by facing target sputtering

1997 J. Phys.: Condens. Matter 9 8547

(http://iopscience.iop.org/0953-8984/9/40/020)

J. Phys.: Condens. Matter **9** (1997) 8547–8552. Printed in the UK PII: S0953-8984(97)80225-1

$(Fe, Co)_{16}N_2$ films with high saturation magnetization prepared by facing target sputtering

H Y Wang and E Y Jiang

Department of Applied Physics, Tianjin University, Tianjin, 300072, People's Republic of China

Received 10 December 1996, in final form 6 June 1997

Abstract. FeCoN films with 10 at.% Co content were prepared by facing target sputtering. The effect of *in situ* annealing and post-deposition annealing on the structure and magnetic property of FeCoN films was investigated. The phases formed in FeCoN films are strongly dependent on the thermal treatment process. Growth at 150 °C, followed by annealing at this temperature, yields the formation of γ'-$(Fe, Co)_4N$ phase, and post-deposition annealing, at 150 and 200 °C, of films grown at room temperature (RT) yields the formation of α'' phase. The film grown at RT followed by annealing at 150 °C exhibits a high saturation magnetization up to 2.7 T. The saturation magnetization of α'' alloy phase is expected to be 2.8–2.9 T, which is as large as that of α''-$Fe_{16}N_2$ reported by Sugita *et al*, and this indicates that appropriate Co addition is not likely to reduce the high magnetization of the α'' alloy phase.

1. Introduction

Since the discovery of an abnormally high magnetization (2.83 T) in α''-$Fe_{16}N_2$ by Kim and Takahashi [1], a lot of intensive work has been done to clarify the physical properties of α''-$Fe_{16}N_2$. The reported values of the saturation magnetization ($4\pi M_s$) range from about 3 T [2, 3] or 2.5–2.8 T [4–7] to almost the same as that for α-Fe [8]. Moreover, there have been several theoretical studies [9–12] to expound the high saturation magnetization. However, no calculation based on band structure can successfully explain the giant magnetization and the theory of its origin is still mysterious.

We consider that such a contradiction is mainly caused by ambiguity in the phase identification of the α''-$Fe_{16}N_2$ compound and the unreliable method for fixing the volume fraction of α''-$Fe_{16}N_2$ phase in the whole film.

In our previous study, we described the preparation of Fe–N films containing the α''-$Fe_{16}N_2$ phase [13] and epitaxial growth of α''-$Fe_{16}N_2$ single-crystal films by facing target sputtering [14]. In the present study, in order to see the relation between the structure and magnetic properties of α'' phase, the Fe–N system is extended to the Fe–Co–N system. From the physical point of view, it is interesting to know whether the high saturation magnetization for α''-$Fe_{16}N_2$ is reduced or not for $(Fe, Co)_{16}N_2$ films. The following four points are considered in choosing Co as the alloy element. (i) bcc structure is stably formed up to a composition of 75 at.% at room temperature; this is essential because α''-$Fe_{16}N_2$ has an analogous bct structure [15]. (ii) The lattice constant a of Fe–Co alloys shows an almost constant value up to a Co content of 30 at.%. (iii) The magnetic moment of Fe–Co alloys increases with increasing Co content and takes a maximum of $2.46\mu_B$ at 30 at.% Co [16]. (iv) The chemical affinity of Co for N is weaker than that of Fe.

0953-8984/97/408547+06$19.50

FeCoN films with 10 at.% Co content were prepared by facing target sputtering (FTS). The effects of *in situ* annealing and post-deposition annealing treatment on the structure and magnetic properties of FeCoN films were studied. The vibrating sample magnetometer (VSM) measurement shows that the FeCoN film post-deposition annealed at 150 °C exhibits a high saturation magnetization $4\pi M_s = 2.7$ T, which gives support to that reported by Sugita *et al* [2, 17, 18], and this indicates that appropriate Co addition is not likely to reduce the high saturation magnetization of the α'' phase.

2. Experiment

The FeCoN films were prepared by FTS onto an NaCl(100) single crystal with a freshly cleaved surface. The lattice constant of NaCl is 0.563 nm, which is smaller by only 1.6% than that of the *a* axis of α''-$Fe_{16}N_2$ (0.572 nm). This provides the possibility of epitaxial growth. The sputtering targets are composite materials consisting of 30 mm × 15 mm Co chips placed on 100 mm diameter × 50 mm Fe (99.99%) targets. The sputtering gas and reactive gas were Ar (99.99%) and N_2 (99.99%) respectively. After the chamber was evacuated to a base pressure of 6×10^{-5} Pa, Ar gas was introduced. During sputtering, the Ar and the N_2 gas pressures were kept at 0.3 and 0.04–0.06 Pa, respectively. The composition of the FeCoN films was adjusted by varying the number of Co chips mounted on Fe targets. The deposition rate was about 0.2 nm s^{-1}. The thickness of the film was about 50 nm. For *in situ* annealing, the substrate was held at sputtering temperature for 30 min. For post-deposition annealing, the film was deposited at room temperature (RT) and subsequently annealed at 150 or 200 °C for 30 min. All annealing processes were carried out under a base vacuum of better than 5×10^{-4} Pa.

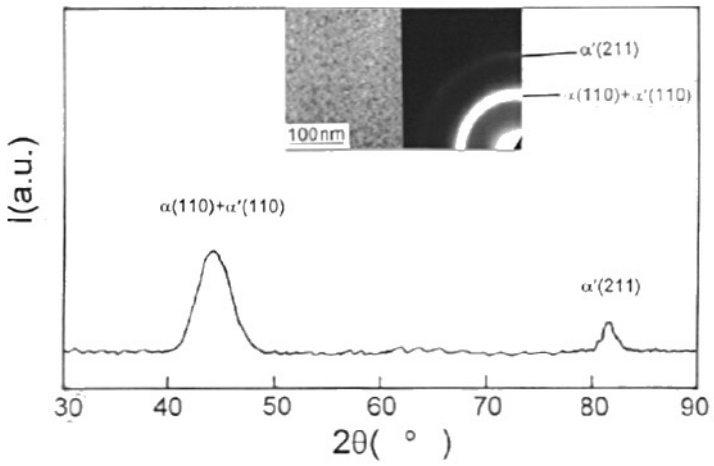

Figure 1. The XRD pattern and TEM BF image and SAD pattern of the FeCoN film with 10 at.% Co content deposited onto NaCl(001) substrates at $p_{N_2} = 0.04$–0.06 Pa and at T_s =RT.

The crystal structures of the FeCoN films were examined with an x-ray diffractometer (XRD) using Cu Kα radiation and a JEM-200CX transmission electron microscope (TEM) capable of energy dispersive x-ray (EDX) analysis. The saturation magnetization was measured at room temperature by VSM with a resolution of 2×10^{-6} emu in an external magnetic field of 5 kOe, which was applied parallel to the sample plane. The total error

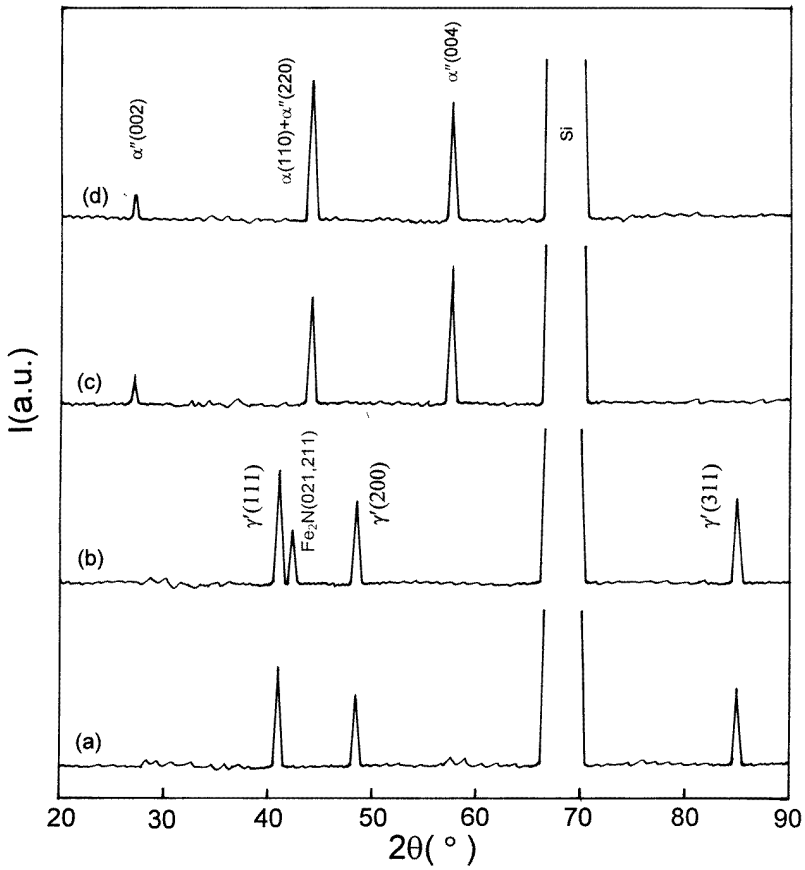

Figure 2. XRD patterns of FeCoN films with 10 at.% Co content on Si(001): (a) film grown onto substrate held at 150 °C during growth then maintained at 150 °C for 30 min; (b) film grown onto substrate held at 200 °C during growth then maintained at 200 °C for 30 min; (c) film grown at RT then annealed at 150 °C for 30 min; (d) film grown at RT then annealed at 200 °C for 30 min.

involved in the measurement of the magnetization was safely estimated to be no more than 6%. The thickness of the film was measured by the multi-beam interference technique. The composition was evaluated using XPS and electron probe analysis.

3. Results and discussion

To determine the influence of the annealing behaviour on the structure and magnetic properties of FeCoN films, the concentration of Co was kept at 10 at.%. The effects of Co concentrations on the structure and magnetic properties of FeCoN films will be reported in another paper in detail.

Figure 1 shows the XRD and TEM bright-field (BF) image and selected area diffraction (SAD) patterns of the FeCoN film with 10 at.% Co content deposited onto NaCl(001) substrates at RT. In the XRD pattern, only α(110) and (211) peaks are observed: no evidence was found for Co–N or Fe–N compounds. The (110) and (211) peak broadening could be due to peak splitting associated with the tetragonal distortion of α-Fe by interstitial

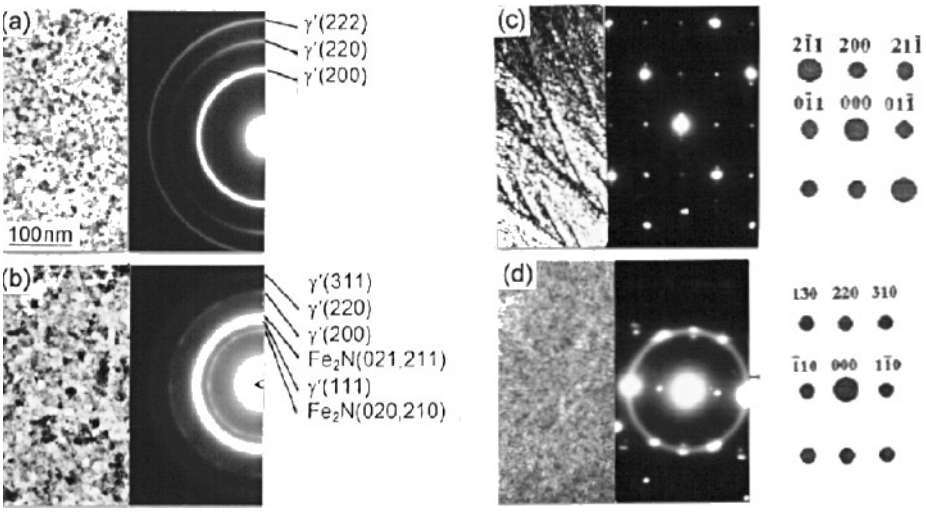

Figure 3. TEM BF images and SAD patterns of FeCoN films corresponding to figure 2(a)–(d).

nitrogen atoms and the formation of the α' martensite phase. The SAD pattern shows a thick polycrystalline ring around the $\alpha(110)$ ring. This is due to the distribution of lattice constants in addition to the smaller crystallite size and a mixture of α-Fe and α' martensite phase co- existing in the film. The grain size estimated from the BF images of the film was about 2–5 nm.

Figure 2 shows the dependence of the XRD patterns of FeCoN films with 10 at.% Co content grown onto Si(001) substrates on annealing conditions. For the samples grown onto a substrate held at 150 °C during growth then maintained at 150 °C for 30 min, i.e., *in situ* annealed at 150 °C for 30 min, the XRD pattern contains γ' peaks; no α'' peaks appear, showing that the film contains γ' only, and that no α'' phase is present in the film (figure 2(a)). Figure 2(b) shows the XRD pattern of the FeCoN film *in situ* annealed at 200 °C for 30 min. It contains γ' and Fe_2N peaks. The three strong peaks are $\gamma'(111)$, (311) and (200), indicating that the γ' phase is the dominant phase (figure 2(b)). For the samples grown at RT then annealed at 150 and 200 °C for 30 min, i.e., post-deposition annealed at 150 and 200 °C, strong diffraction peaks of α'' phase are observed, and no γ' peaks appear in the XRD patterns. This shows that the α'' phase is the dominant phase in the two post-deposition annealed films. The intensity of α'' phase in figure 2(c) is stronger than that in figure 2(d), but the intensity of the $\alpha(110)$ peak in figure 2(d) is stronger than that in figure 2(c), indicating that the amount of α phase is larger in the film post-deposition annealed at the higher temperature.

For reliable phase identification in FeCoN films, TEM was used to characterize the crystal structure and morphology for all the above-mentioned specimens. Figure 3 shows the BF images and the SAD patterns corresponding to the specimens in figure 2. For the film *in situ* annealed at 150 °C, the SAD pattern shows that the film contains γ' phase only. A uniform density of the intensity distribution present in the SAD pattern indicates that the microstructure of the film is composed of randomly oriented polycrystalline grains. The grain sizes estimated from the BF images of the films are around 8–12 nm. For the sample *in situ* annealed at 200 °C, there are Fe_2N and γ' phases identified in the SAD pattern, as shown in figure 3(b). The SAD pattern exhibits some discontinuous diffraction rings with bright spots, showing that the film is polycrystalline and there emerges some texture

Table 1. Phase and saturation magnetization of FeCoN films: dependence on *in situ* and post-deposition annealing temperature.

Annealing temperature (°C)	All phases	Dominant phases	$4\pi M_s$ (T)
T_s[a] = RT	$\alpha' + \alpha$	α'	2.2
T_s[b] = 150	γ'	γ'	1.8
$T_s = 200$	$\gamma' + Fe_2N$	γ'	1.5
$T_a = 150$	$\alpha + \alpha''$	α''	2.7
$T_a = 200$	$\alpha + \alpha''$	α''	2.6

[a] The temperature of the substrate during growth and subsequent *in situ* annealing.
[b] The temperature of post-growth annealing; the growth temperature was RT for these cases.

and specific orientation relationship in the film. From the BF image, one can see that the crystallite size is in the range of 15–20 nm, which is larger than that of the films deposited at lower temperatures. For the sample post-deposition annealed at 150 °C, the SAD pattern consists of α single-crystal spots and single-crystal spots of α'' phase, which is indexed as in the [011] direction in reciprocal space. For the sample post-deposition annealed at 200 °C, the SAD pattern contains an $\alpha(110)$ ring and single-crystal spots of α'' phase, which is indexed as in the [001] direction in reciprocal space. The superlattice reflections from (110), (011), (200), (220) and (211) of the α'' phase are clearly observed. Using these superlattice reflections, determined values of lattice constants $a = 0.574 \pm 0.002$ nm and $c = 0.630 \pm 0.004$ nm of the α'' phase are almost equal to the results obtained by Jack [15]. This indicates that the Co containing α'' alloy phase has the same structure as the α''-$Fe_{16}N_2$ phase. EDX analysis was carried out on the same area as the SAD to determine the composition of the SAD area in the film. The composition of the area was determined to be 79 at.% Fe, 10 at.% Co and 11 at.% N. There are no diffraction spots or rings of Fe–Co or Co–N compounds in the SAD patterns. Therefore the phase corresponding to the single-crystal spots in the SAD was determined to be a Co containing 16:2 nitride, which can be denoted by α''-$(Fe, Co)_{16}N_2$.

From figures 2 and 3, one can see that the effect of sputtering temperature during the film deposition, i.e., *in situ* annealing, on the structure is substantially different from that of post-deposition annealing. The experiment shows that RT deposition followed by annealing is an effective method of achieving the α'' alloy phase. For *in situ* annealing, the substrate temperature could influence the combination of the atoms on the surface of the substrate, and at a higher substrate temperature the atoms on the substrate behave more actively, so it is more likely to form γ'-$(Fe, Co)_4N$ and $(Fe, Co)_2N$ with a high stability. The lack of α'' alloy phase growth was attributed to the more stable growth of γ'-$(Fe, Co)_4N$ and $(Fe, Co)_2N$. For post-deposition annealing, the annealing temperature could influence the ordering process of nitrogen atoms in α' martensite. According to Jack [15], in the α' martensite phase, nitrogen atoms randomly occupy the octahedral interstices. The α'' phase has an ordered nitrogen site location of the octahedral interstices. The crystal structure of α''-$Fe_{16}N_2$ is bct ($a = 0.5728$ nm, $c = 0.629$ nm), so α''-$Fe_{16}N_2$ can be described as a martensite with an ordered distribution of nitrogen atoms in the deformed octahedral interstices. The post-deposition annealing treatment, needed to order the nitrogen atoms in the alloy, must be very gentle to prevent the stable compound forming. We found that a good annealing temperature was 150–180 °C.

Table 1 shows the dependence of different phases and saturation magnetization of FeCoN films with 10 at.% Co on *in situ* and post-deposition annealing temperature. The two post-

deposition annealed films, in which α'' alloys phase gathered, have $4\pi M_s = 2.6$–2.7 T, which is larger than that of Fe–Co alloy with 30 at.% Co (2.4 T). The $4\pi M_s$ value of the α'' phase is expected to be 2.8–2.9 T, which is in accordance with the results of Kim and Takahashi [1] and Komuro and co-workers [17]. The saturation magnetization of the α''-$(Fe, Co)_{16}N_2$ phase is as large as that of α''-$Fe_{16}N_2$, indicating that proper Co addition does not induce notable changes in the giant magnetic moment of α''-$Fe_{16}N_2$. The films deposited and *in situ* annealed at 150 and 200 °C do not have the same saturation magnetization as those deposited at RT and post-deposition annealed at 150 and 200 °C. The reason is that α' martensite is the dominant phase in the film deposited at RT and γ' phase is the dominant phase in the two *in situ* annealed films, as shown in figures 1 and 2.

4. Conclusion

FeCoN films with 10 at.% Co content were prepared by facing target sputtering. The effects of *in situ* annealing and post-deposition annealing on the structure and magnetic properties of FeCoN film are quite different. The phases formed in FeCoN films are quite diversified by *in situ* and post-deposition annealing temperature. The film *in situ* annealed at 150 °C yields the formation of γ'-$(Fe, Co)_4N$ phase, and that post-deposition annealed at 150 °C yields the formation of the α'' alloy phase, so post-deposition annealing is more advantageous than *in situ* annealing to obtain the α'' alloy phase. The film post-deposition annealed at 150 °C exhibits a high saturation magnetization up to 2.7 T. The saturation magnetization of the α'' alloy phase is expected to be 2.8–2.9 T, which is as large as that of α''-$Fe_{16}N_2$ reported by Sugita *et al* [2], and this indicates proper Co addition is not likely to reduce the high saturation magnetization of the α'' alloy phase.

Acknowledgments

This work is supported in part by the National Natural Science Foundation of China and Zhongguanchun Union Measurement Foundation. The authors are grateful to Dr Y P Wang and others in the TEM Laboratory of Peking University.

References

[1] Kim T K and Takahashi M 1972 *Appl. Phys. Lett.* **20** 492
[2] Sugita Y, Takahashi H, Komuro M, Mitsuoka K and Sakuma A 1994 *J. Appl. Phys.* **76** 6637
[3] Gao C and Doyle W D 1993 *J. Appl. Phys.* **73** 6579
[4] Nakajima K, Okamoto S and Okada T 1989 *J. Appl. Phys.* **65** 4357
[5] Ortiz C, Dumpich G and Morrish A H 1994 *Appl. Phys. Lett.* **65** 2737
[6] Jiang H, Tao K and Li H 1994 *J. Phys.: Condens. Matter* **6** L279
[7] Wallance W E and Huang M Q 1994 *J. Appl. Phys.* **76** 6648
[8] Takahashi M, Shoji H, Nashi H, Wakiyama T, Doi M and Matsui M 1994 *J. Appl. Phys.* **76** 6642
[9] Min B I 1992 *Phys. Rev.* B **46** 8232
[10] Coehoorn R, Daalderop G H O and Jansen H J F 1993 *Phys. Rev.* B **48** 3830
[11] Coey J M D *et al* 1994 *J. Phys.: Condens. Matter* **6** L23
[12] Sakuma A and Sugita Y 1993 *Mater. Res. Soc. Symp. Proc.* vol 313 (Pittsburgh, PA: Materials Research Society) 257
[13] Sun D C, Jiang E Y, Liu M S and Lin C 1995 *J. Phys. D: Appl. Phys.* **28** 4
[14] Sun D C, Lin C and Jiang E Y 1995 *J. Phys.: Condens. Matter* **7** 3667
[15] Jack K H 1951 *Proc. R. Soc.* A **208** 216
[16] Bozorth R M 1993 *Ferromagnetism* (New York: IEEE)
[17] Komuro M, Kozono Y, Hanazono M and Sugita Y 1990 *J. Appl. Phys.* **67** 5126
[18] Sugita Y, Mitsuoka K, Komuro M, Hoshiya H, Kozono Y and Hanazono M 1991 *J. Appl. Phys.* **70** 5977